Original article

Efficient removal of Pb(II) from water using silica gel functionalized with thiosalicylic acid: Response surface methodology for optimization

Nafisur Rahman [a,*], Mohd Nasir [a], Poornima Varshney [a], Abdullah M. Al-Enizi [b,*], Mohd Ubaidullah [b], Shoyebmohamad F. Shaikh [b], Mohammed A. Al-Adrabalnabi [b]

[a] Department of Chemistry, Aligarh Muslim University, Aligarh 202002, India
[b] Department of Chemistry, College of Science, King Saud University, Riyadh 11451, Saudi Arabia

A B S T R A C T

The adsorption of Pb(II) onto silica gel functionalized with thiosalicylic acid (TSA@)amine modified SiO_2) was studied at 300, 305, 310 and 315 K. The effects of independent variables (pH, adsorbent dose and initial concentration of Pb(II)) on the removal of Pb(II) from water were evaluated and response surface methodology was applied to optimize them. Under the optimized conditions (pH: 6; adsorbent dose, 0.20 g/20 mL and initial concentration: 50 mg/L), removal efficiency of Pb(II) was 98.78%. The adsorption equilibrium data obtained from batch experiments were examined by various isotherm models. Freundlich isotherm model fitted well to the experimental data and indicating the multilayer coverage of Pb(II) on the heterogeneous surface of TSA@)amine modified SiO_2. Adsorption kinetic data were investigated by surface and diffusion based kinetic models. Kinetic data fitted well to pseudo-second order model with $R^2 > 0.999$. Elovich model with $R^2 > 0.999$ revealed the occurrence of chemical reaction between Pb(II) and active sites of TSA@)amine modified SiO_2. Thermodynamic parameters suggested the spontaneous and endothermic nature of Pb(II) adsorption onto TSA@)amine modified SiO_2.

1. Introduction

The operation of modern chemical industries produces plenty of wastewater containing heavy metal ions and organic pollutants which have led to the emergence of serious problems of water pollution (Zhou et al., 2020; Ibrahim et al., 2020). The heavy metals are non-degradable in environment and can enter human body via food chain and drinking water. Among the heavy metal ions, Pb(II) has received much attention because of its acute toxicity (Kumar et al., 2020; Levin et al., 2020). Excessive exposure of human body to Pb(II) ions causes neurological, hematological, gastrointestinal, cardiovascular and reproductive disorders (Debnath et al., 2019). The presence of high level of Pb(II) in blood causes disturbance in the functioning of central nervous system and there-

fore, leads to encephalopathy and edema which affects the cerebellum (Rao et al., 2014). The accumulation of lead even at a low concentration can damage the nerves (Fewtrell et al., 2003). Thus, the removal of Pb(II) from surface water and groundwater is an important task to protect the public health and environment. For the purification of water, a variety of techniques such as coagulation (Tang et al.,2016), membrane filtration (Almasian et al., 2018), reverse osmosis (Thaci and Gashi, 2019), solvent extraction (Joel et al., 2020), ion exchange (Lutfullah et al., 2012a, 2012b) and adsorption (Gupta et al., 2004; Rahman et al., 2017) has been proposed. Among them, adsorption is a simple, low cost and effective method because of availability of different types of adsorbent and their easy regeneration for reuse (Qin et al., 2020). Recently, carbonized *Phoenix dactylifera* seed has been used to remove Pb(II) from groundwater samples in Oman. The adsorption capacity of date stone was 9.03 mg/g for Pb(II) ions (Azmi et al., 2020). The soy waste biomass functionalized with sulphur based chelating agent was studied to removal of Pb(II) and its efficiency was much higher as compared to soy waste biomass (Bulgariu and Bulgariu, 2018). Activated carbon derived from *Manilkarazapota* tree-wood was found to be a suitable adsorbent for uptake of Pb(II). The adsorption process was explained by Langmuir isotherm model (Sujatha et al., 2020). Additionally, the valorization possibilities of exhausted biosorbents loaded with metal ions have been

explored and their advantages and disadvantages were also discussed (Badescu et al., 2018).

Currently, response surface methodology (RSM) is used for optimization of selected variables of any process or method to achieve the best response instead of conventional methods due to its time consuming ability and unable to provide interactive effects of variables on the response (Khammar et al., 2020). RSM has been applied to optimize the variables of adsorption process (Rahman and Nasir, 2019; Rahman et al., 2020).

To understand the behaviour of the adsorption of solute on the surface of the adsorbent under optimized experimental conditions the experimental data were critically examined by adsorption isotherm models (Rahman et al., 2015). These isotherm studies provided the information related to the nature of interaction between adsorbate and the surface of the adsorbent. Similarly, kinetic models were used to characterize the dynamics of the adsorption process and to explain the mechanism of adsorption process (Rahman and Khan, 2016).

Researchers have generally used linear regression analysis of isotherm and kinetic equations to judge the best fitted model (Rahman and Haseen, 2014; Rahman and Khan, 2015). However, the original adsorption isotherm and kinetic equations have been manipulated to transform them into linear equations. These manipulations have been criticized due to the violation of fundamental aspects of the original theories (Kumar and Sivanesan, 2006). Adsorption isotherm and kinetics parameters can be obtained by nonlinear regression analysis using an appropriate software without ignoring the basic concepts of the models. Such results ultimately increase the accuracy and reliability to find the model which best fit to the experimental data.

In our previous study, the synthesis and characterization of silica gel functionalized with thiosalicyclic acid (TSA@)amine modified SiO_2) was reported (Rahman and Nasir, 2020). In this study, the potential ofTSA@)amine modified SiO_2 was examined for the uptake of Pb(II) from water. The process variables such as pH, adsorbent dose and initial concentration of Pb(II) were optimized by RSM via Box-Behnken design (BBD). The adsorption equilibrium data were examined by Langmuir, Freundlich, and Temkin isotherm models. The adsorption kinetic data were investigated by surface-based and diffusion-based kinetic models. The thermodynamic parameters were calculated to explore the feasibility and spontaneity of the uptake of Pb(II).

2. Experimental

2.1. Materials

Silica gel (Merck, India), 3-aminopropyltrimethoxysilane (Sigma Aldrich) and thiosalicylic acid (HiMedia Laboratories, India) were used to prepare the adsorbent. Lead (II) nitrate, sodium hydroxide pellets and HCl were procured from Merck, India.

2.2. Instrumentation

Atomic absorption spectrometer (AAS) (GBC Scientific, Australia) and digital pH meter (Eutech instruments, Singapore) were employed to measure the Pb(II) concentration and solution pH, respectively. Water bath shaker with variable speed and temperature control was used to agitate the solution mixture.

2.3. Synthesis of TSA@ amine modified SiO_2

The synthesis of TSA@ amine modified SiO_2 was carried out according to the method reported in the literature (Rahman and Nasir, 2020).

2.4. Experimental design for optimization

RSM via BBD was employed to optimize the influencing operating parameters for the removal of Pb(II). Design Expert (trial version 11.1.0.1) Software was used to generate BBD matrix, regression analysis and 3D response surface plots for the optimization of variables of adsorption process. In BBD, the number of experimental runs required is less than those for central composite design and thus, reducing the consumption of chemicals in the optimization process. In the present study, three independent factors namely, pH (X), adsorbent dose (Y) and initial concentration (Z) of Pb(II) were selected and each factor was investigated at three levels (high (+1), central point (0) and low (−1)) which are given in Table S1 (Supplementary information). BBD matrix suggested a total 17 sets of preliminary experiments involving different combinations of independent variables to achieve the best response (percent removal). BBD matrix is presented in Table 1.

RSM was applied to optimize influencing factors by using the data obtained from the experimental design for the removal efficiency of Pb(II) as a response (% R) and the empirical relation between the response and the independent factors were evaluated by the second order polynomial equation.

2.5. Adsorption isotherms

In order to study the adsorption isotherms, experiments were conducted under the optimal conditions (pH: 6; adsorbent dose: 0.20 g) using different concentrations of Pb(II) and temperatures. In this study, 20 mL solutions of different concentration of Pb(II) (10–100 mg/L) maintained at pH 6 were transferred to a series of 50 mL conical flasks. To each flask, TSA@ amine modified SiO_2 (0.20 g) was added and the mixture was agitated (125 rpm) at a desired temperature (300–315 K) in a shaker for 50 min. The adsorbent was removed by filtration and the Pb(II) content in the filtrate was determined by AAS. For AAS determination, calibration curve was constructed using standard solution of Pb(II) in the range of 1–20 mg/L. The detection limit of the AAS instrument was 0.01 mg/L. The adsorbed amount at equilibrium, q_e (mg/g) and removal efficiency, R (%) were computed using Eqs. (1) and (2):

$$q_e = \frac{(C_0 - C_e)V}{M} \tag{1}$$

$$R(\%) = \frac{C_0 - C_e}{C_0} \times 100 \tag{2}$$

where C_0 and C_e are initial and equilibrium Pb(II) concentration (mg/L) in the solution, respectively. M and V represent mass of the adsorbent (g) and solution volume (L), respectively.

2.6. Adsorption kinetics

The kinetic experiments were performed in batch mode. In general, 0.20 g of TSA@amine modified SiO_2 was mixed with 20 mL of Pb(II) solution (50 mg/L; pH 6.0) in a series of Erlenmeyer flasks. The resulting solutions were agitated (125 rpm) in temperature-controlled shaker at the desired temperature (300–315 K). Conical flasks were withdrawn from the water bath at different time intervals and then solutions were separated from the adsorbent. Finally, the residual Pb(II) content was estimated by AAS and then adsorbed amount (q_t, mg/g) of Pb(II) onto TSA@amine modified SiO_2 at predetermined time intervals was computed.

2.7. Evaluation of error functions

The values of correlation coefficient (R^2) are not sufficient to judge the best fitted model. Therefore, different statistical error

Table 1
Box-Behnken design matrix with experimental and predicted values.

Exp. Run	X	Y	Z	Removal (%) Observed	Removal (%) Predicted
1	6	0.2	50	98.78	98.78
2	6	0.2	50	98.78	98.78
3	10	0.2	20	20.68	20.28
4	6	0.2	50	98.78	98.78
5	6	0.3	20	89.35	89.23
6	2	0.2	20	14.62	14.83
7	6	0.3	80	67.47	67.17
8	6	0.1	20	50.82	51.12
9	10	0.3	50	29.11	29.63
10	10	0.1	50	3.16	3.25
11	2	0.2	80	8.24	8.64
12	2	0.3	50	29.04	28.95
13	6	0.1	80	51.77	51.89
14	6	0.2	50	98.78	98.78
15	6	0.2	50	98.78	98.78
16	10	0.2	80	5.40	5.19
17	2	0.1	50	2.46	1.94

functions were calculated to validate the adequacy of the isotherm and kinetic models. The equations of the chosen error functions are mentioned in Table 2.

3. Results and discussion

3.1. Model validation

The experiments were conducted according to the BBD matrix and percent removal of Pb(II) was determined (Table 1). The results were examined by different regression models (Linear, interactive and quadratic models) and statistical parameters are presented in Table S2 (Supplementary Information). Quadratic model was selected based on lower p-value, high F-value, minimum predicted residual sum of square value and highest R^2 value. The second degree polynomial quadratic model that correlates the response to the selected variables can be given by Eqs. (3) and (4) in terms of coded and actual factors, respectively.

In coded factors

$$R(\%) = +98.78 + 0.4992\,X + 13.35\,Y - 5.32\,Z - 0.1585\,XY - 2.23\,XZ - 5.71\,YZ - 67.73\,X^2 - 15.11\,Y^2 - 18.82\,Z^2 \tag{3}$$

In actual factors

Table 2
Mathematical equations of error functions.

Error function	Abbreviation	Expression
Average relative error deviation	ARED	$\frac{100}{N}\sum_{i=1}^{N}\left|\frac{q_{e,exp}-q_{e,cal}}{q_{e,exp}}\right|_i$
Sum of squares of the error	SSE	$\sum_{i=1}^{N}\left(q_{e,cal}-q_{e,exp}\right)_i^2$
Sum of the absolute error	SAE	$\sum_{i=1}^{N}\left|q_{e,cal}-q_{e,exp}\right|_i$
Chi-square statistic	χ^2	$\sum_{i=1}^{N}\frac{\left(q_{e,exp}-q_{e,cal}\right)^2}{q_{e,cal}}$

$q_{e,cal}$ and $q_{e,exp}$ are the calculated and experimental adsorption capacities (mg/g) at equilibrium. N represents experimental data points.

$$\begin{aligned}R\,(\%) =\ & -209.94940 + 51.92715\,\text{pH} \\ & + 835.37750\,\text{adsorbent dose} \\ & + 2.40507\,\text{initial concentration} - 0.396250\,\text{pH} \\ & * \text{adsorbent dose} - 0.018542\,\text{pH} \\ & * \text{initial concentration} - 1.90250\,\text{adsorbent dose} \\ & * \text{initial concentration} - 4.23300\text{pH}^2 \\ & - 1511.05000\,\text{adsorbent dose}^2 \\ & - 0.020908\,\text{initial concentration}^2 \end{aligned} \tag{4}$$

The results of analysis of variance (ANOVA) were used to examine the significance of the model terms (Table 3). Model terms are considered as significant when p-value < 0.05 and F-value greater than the value of standard distribution table for a given degree of freedom at 95% confidence level. In the present study the high F-value (16504.65) and p-value < 0.0001 of the quadratic model illustrated its suitability and adequacy. The reliability of the quadratic model for prediction of response was judged by the adequate precision which is the signal to noise ratio and its high value (308.3165) pointed towards the adequate signal and confirming the goodness of the model (Chowdury, et al., 2016). The p-value for lack-of-fit was not given by the software but it was suggested that the lack-of-fit is insignificant. Further, the low value of coefficient of variance (0.8039%) and high correlation coefficient value (R^2 = 0.9999) suggested the accuracy and precision of the developed model. It was found that if the difference between the values of correlation coefficient (R^2) for the adjusted and predicted response is<0.20, then it would be a reasonable agreement between them. Herein, the difference between adjusted R^2 (0.9999) and predicted R^2 (0.9992) is < 0.20 which indicated closeness between predicted and experimental values (Fig. S1, Supplementary information). Moreover, the model term XY is not significant because its p-value is 0.4642. Therefore, the contribution of model term XY can be ignored and modified second order polynomial quadratic model in coded and actual factors are represented by Eqs. (5) and (6), respectively.

$$R(\%) = +98.78 + 0.4992\,X + 13.35\,Y - 5.32\,Z - 2.23\,XZ - 5.71\,YZ - 67.73\,X^2 - 15.11\,Y^2 - 18.82\,Z^2 \tag{5}$$

Table 3
ANOVA for quadratic model.

Source	Sum of Squares	df	Mean Square	F-value	p-value	
Model	24913.20	9	2768.13	16504.65	<0.0001	significant
X-pH	1.99	1	1.99	11.89	0.0107	
Z-Adsorbent dose	1424.82	1	1424.82	8495.30	<0.0001	
C-Initial concentration	226.74	1	226.74	1351.90	<0.0001	
XY	0.1005	1	0.1005	0.5992	0.4642	
XZ	19.80	1	19.80	118.07	<0.0001	
BC	130.30	1	130.30	776.91	<0.0001	
X^2	19314.03	1	19314.03	1.152E + 05	<0.0001	
Y^2	961.38	1	961.38	5732.09	<0.0001	
Z	1490.86	1	1490.86	8889.07	<0.0001	
Residual	1.17	7	0.1677			
Lack of Fit	1.17	3	0.3913			Insignificant
Pure Error	0.0000	4	0.0000			
Cor Total	24914.38	16				

$$\begin{aligned} R\ (\%) = &-209.94940 + 51.92715\ \text{pH} \\ &+ 835.37750\ \text{adsorbent dose} \\ &+ 2.40507\ \text{initial concentration } - 0.018542\ \text{pH} \\ &* \text{initial concentration} - 1.90250\ \text{adsorbent dose} \\ &* \text{initial concentration} - 4.23300\text{pH}^2 \\ &- 1511.05000\ \text{adsorbent dose}^2 \\ &- 0.020908\ \text{initial concentration}^2 \end{aligned} \quad (6)$$

3.2. Response surface analysis

The regression equation is graphically represented by 3-D response surface plots (Fig. 1). Fig. 1a shows the interactive effect of pH (X) and initial concentration (Z) on the removal (% R) when adsorbent dose (Y) was fixed at center point (Y = 20 mg and contact time 50 min). It was observed that the removal (%) at any fixed pH, increases with increasing the initial concentration upto 50 mg/L and maximum removal efficiency (98.78%) was achieved at contact time of 50 min. Further increase in Pb(II) ion concentration showed a decreasing trend in removal efficiency due to unavailability of binding sites on the surface of TSA@amine modified SiO$_2$. The interaction effect of adsorbent dose (Y) and initial concentration (Z) while keeping the pH (X) at the center point on the removal efficiency revealed that the removal efficiency increases from 51.77% to 98.78% with increasing the amount of TSA@amine modified SiO$_2$ from 0.10 g to 0.20 g. Further increase in the amount of adsorbent did not improve the removal efficiency. Hence the maximum removal was achieved with 0.20 g of TSA@amine modified SiO$_2$. This resulted due to the increase in the surface area and number of active sites to bind with Pb(II) ions (Fig. 1b).

3.3. Adsorption isotherms

The equilibrium data for the uptake of Pb(II) onto TSA@)amine modified SiO$_2$ were applied to Langmuir, Freundlich, and Temkin isotherm models for proper description of the nature of interaction between Pb(II) and the adsorbent. Table 4 shows the nonlinear equations of the studied isotherm models. Error functions such as ARED, SSE, SAE and χ^2 were calculated to validate the best fit isotherm model (Table 4). The nonlinear isotherm parameters were computed by using Microsoft Excel SOLVER function spread sheet method (Rahman and Nasir, 2018) and results are presented in Table 4. The nonlinear fit(q_e (mg/g) predicted versus C_e (mg/L))
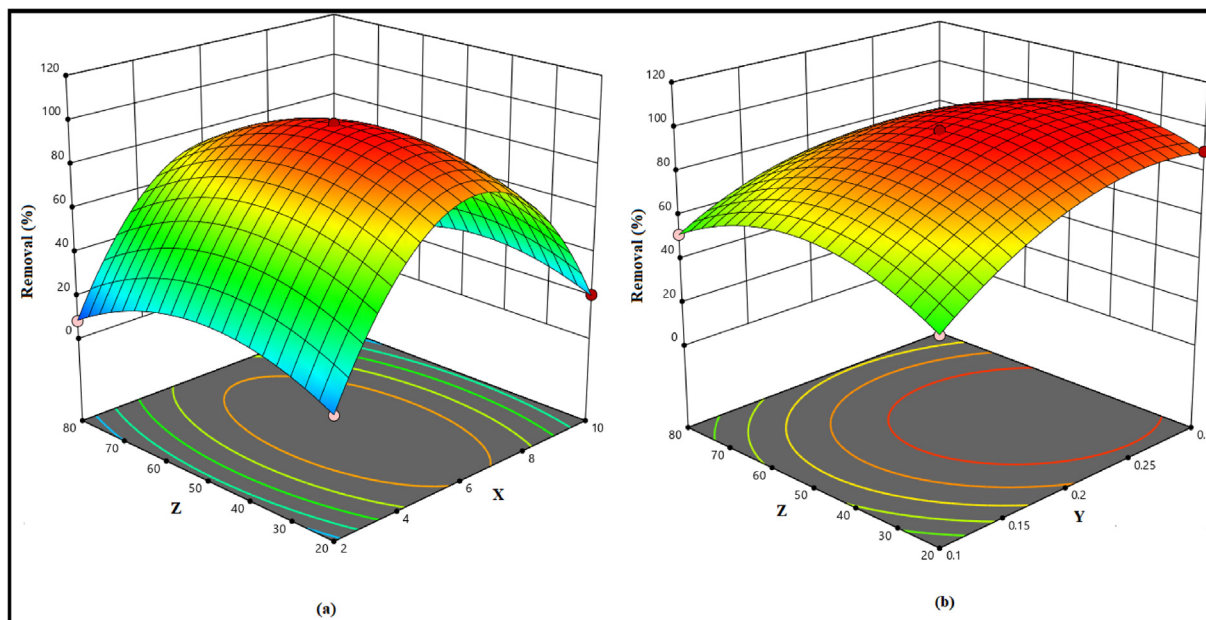

Fig. 1. Response surface plots to show the effects of (a) pH and initial concentration and (b) adsorbent dose and initial concentration on the percentage removal of Pb(II).

Table 4

Equations and parameters of isotherm models for the adsorption of Pb (II) onto TSA@amine modified SiO_2.

Isotherm Model	Nonlinear equation	Temp (K)	Parameters			Error function			
			q_e (mg/g)	K_L	R^2	ARED	SSE	SAE	χ^2
Langmuir	$q_e = \frac{q_m K_L C_e}{1 + K_L C_e}$	300	96.131	0.442	0.9980	0.392	13.170	3.629	0.142
		305	99.156	0.574	0.9950	0.504	22.658	4.760	0.240
		310	104.217	0.831	0.9920	0.779	56.701	7.530	0.586
		315	109.478	1.312	0.9920	1.284	155.177	12.457	1.600
Freundlich	$q_e = K_F C_e^{1/n}$		K_F	n					
		300	92.466	33.113	1.919	0.9992	3.892×10^{-4}	0.001	0.036	1.081×10^{-5}
		305	94.324	39.513	1.996	0.9994	7.627×10^{-4}	0.005	0.072	5.296×10^{-5}
		310	96.409	53.094	2.001	0.9997	2.875×10^{-3}	0.077	0.278	7.963×10^{-4}
		315	97.301	58.221	2.137	0.9998	2.886×10^{-3}	0.078	0.280	8.03×10^{-4}
Temkin	$q_e = \left(\frac{RT}{b_T}\right) ln A_T C_e$		A_T	b_T					
		300	92.359	3.158	84.493	0.9992	1.546×10^{-3}	0.020	0.143	2.162×10^{-4}
		305	94.111	3.655	81.321	0.9993	3.019×10^{-3}	0.081	0.285	8.580×10^{-4}
		310	96.229	5.525	77.974	0.9995	4.737×10^{-3}	0.210	0.458	2.172×10^{-3}
		315	97.528	6.299	76.114	0.9998	5.648×10^{-3}	0.257	0.507	2.649×10^{-3}

q_e: experimental adsorption capacity(mg/g), q_m : calculated adsorption capacity (mg/g), C_e : concentration of Pb (II) in the solution phase at equilibrium (mg L^{-1}), K_L: Langmuir isotherm constant (L/mg), k_F & $\frac{1}{n}$ are Freundlich isotherm constants, A_T & b_T are Temkin isotherm constants related to equilibrium binding constant and adsorption heat, respectively.

*q_e = 92.502, 94.396, 96.687, 97.021 mg/g at 300, 305, 310 and 315 K, respectively (Contact time = 50 min; pH = 6.0; adsorbent dose = 0.20 g).
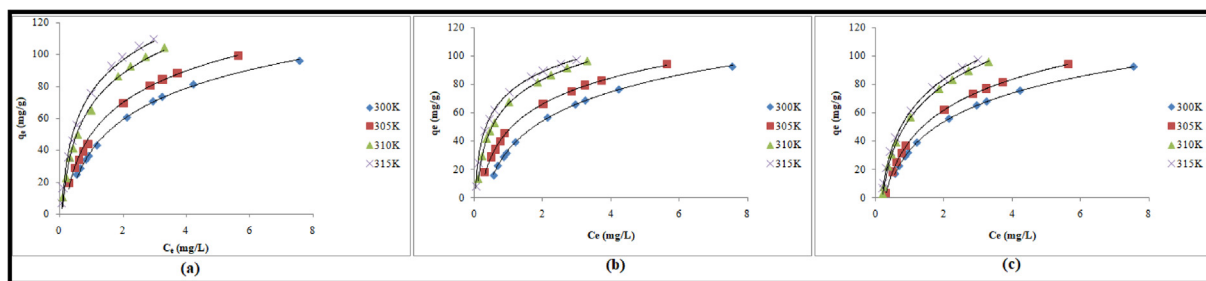
Fig. 2. Nonlinear (a) Langmuir, (b) Freundlich and (c) Temkin isotherm plots for the adsorption of Pb (II) onto TSA@amine modified SiO_2.

of Langmuir, Freundlich and Temkin, models are presented in Fig. 2 (a)–(c), respectively.

The maximum capacities calculated from Langmuir isotherm were 96.131, 99.156, 104.217 and 109.478 mg/g at 300, 305, 310 and 315 K, respectively. The affinity between TSA@)amine modified SiO_2 and Pb(II) was evaluated from the Langmuir isotherm constant (K_L) using dimensionless separation factor, R_L which is defined by Eq. (7) (Rahman and Haseen, 2015):

$$R_L = \frac{1}{1 + K_L C_o} \qquad (7)$$

Where C_o is the initial concentration of Pb(II). For adsorption to occur favourably, it is required that $0 < R_L < 1$. In this study, the values of R_L were in the range of 0.022–0.184, 0.017–0.148, 0.012–0.107 and 0.008–0.071 at 300, 305, 310 and 315 K, respectively which suggested the favorable uptake of Pb(II).

Freundlich isotherm model deals with the multilayer adsorption of solute onto the adsorbent surface. In this model, the parameter $1/n$ is related to the degree of surface heterogeneity. The small value of $1/n$ denotes the more heterogeneous surface while a value near unity suggested that the adsorbent has more homogeneous surface (Chen et al., 2007). The values of $1/n$ obtained for adsorption of Pb(II) onto TSA@)amine modified SiO_2 were 0.521, 0.501, 0.499 and 0.468 at 300, 305, 310 and 315 K, respectively which indicated that the involvement of heterogeneous surface of adsorbent.

Temkin isotherm model assumes that the free energy of adsorption is a function of surface coverage and indicates the adsorbate/adsorbent interaction. The values of A_T were in the range of 3.158–6.299 at the studied temperatures. The values of b_T, heat of adsorp-

tion, were 84.493, 81.321, 77.974 and 76.114 J/mol at 300,305, 310 and 315 K, respectively. The positive values of b_T demonstrated the endothermic nature of adsorption process.

All studied isotherm models exhibit high correlation coefficient ($R^2 > 0.990$) but the best fitting model cannot be judged accurately based on R^2 values only. The maximum adsorption capacities evaluated from Langmuir isotherm model were not closely related to the experimental adsorption capacities. The adsorption capacities obtained from Freundlich and Temkin models were near to the experimental values at all the studied temperatures. Additionally, the values of error functions such as ARED, SSE, SAE and χ^2 were found to be lowest for Freundlich model in comparison to those obtained for Temkin and Langmuir models at 300, 305, 310 and 315 K. Therefore, it was suggested that both Freundlich and Temkin isotherm models are capable to interpret the uptake of Pb(II) ions onto TSA@amine modified SiO_2. Further, the applicability of Freundlich isotherm model suggested that multilayer adsorption of Pb(II) ions occurred on heterogeneous surface of TSA@amine modified SiO_2 and Temkin model revealed the interaction between Pb(II) ion and active surface sites of the adsorbent.
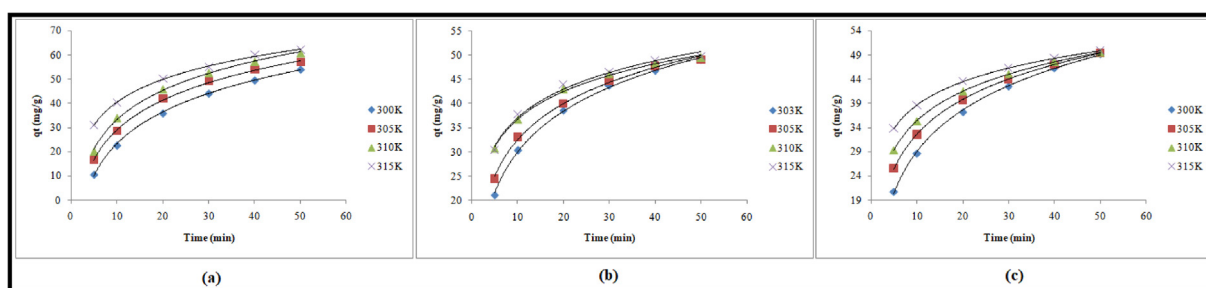
3.4. Adsorption kinetics

Kinetic models such as the pseudo-first order, pseudo-second order, Elovich, and double exponential models were used to study the adsorption kinetic data. The nonlinear equations of pseudo-first order and pseudo-second order kinetic models are presented in Table 5. Nonlinear regression analysis (Rahman and Nasir, 2017, 2020) was performed to determine the kinetic parameters of pseudo-first and pseudo-second order models (Table 5). Fig. 3

Table 5
Nonlinear kinetic equation and parameters for the adsorption of Pb (II) onto TSA@amine modified SiO₂.

Kinetic model	Nonlinear equation	Temp (K)	Parameters			Error function			
			*q_e (mg/g)	k_1(min^{-1})	R^2	ARED	SSE	SAE	χ^2
Pseudo-first order(PFO)	$q_t = q_e(1 - e^{-k_1 t})$	300	54.09	0.046	0.9990	0.104	25.776	5.077	0.526
		305	56.94	0.062	0.9990	0.156	59.290	7.700	1.204
		310	60.81	0.107	0.9982	0.228	127.667	11.299	2.578
		315	62.12	0.201	0.9979	0.249	153.537	12.391	3.088
Pseudo-second order (PSO)	$q_t = \frac{k_2 q_e^2 t}{1 + k_2 q_e t}$			**k_2 (g/mg/min)**					
		300	49.11	0.002	0.9991	0.002	0.008	0.093	1.764×10^{-4}
		305	49.11	0.003	0.9991	0.003	0.016	0.127	3.276×10^{-4}
		310	49.51	0.005	0.9990	0.000	0.000	0.002	0.000
		315	49.78	0.006	0.9990	0.000	0.002	0.048	0.463×10^{-4}
Elovich	$q_t = \frac{1}{\beta} ln(1 + \alpha\beta t)$			**α**	**β**				
		300	49.244	9.701	0.073	0.9990	0.004	0.053	0.231	0.001
		305	49.377	21.010	0.092	0.9991	0.003	0.019	0.140	0.004
		310	49.600	45.999	0.112	0.9997	0.002	0.008	0.087	1.529×10^{-4}
		315	49.951	169.387	0.142	0.9994	0.004	0.050	0.224	0.001

q_e and q_t are adsorption capacities of adsorption (mg/g) at equilibrium and time t, respectively. k_1; rate constant (min^{-1}) of the model (PFO), k_2; PSO rate constant (g/mg/min), α; initial adsorption rate (mg/g min) and β; desorption constant (mg/g) and activation energy for chemisorption,*q_e = 49.01, 49.24, 49.51 and 49.73 mg/g at 300, 305, 310 and 315 K, respectively (C_0 = 50 mg/L; pH 6.0; contact time = 50 min; adsorbent dose = 0.2 g; volume = 20 mL).

Fig. 3. Nonlinear (a) pseudo-first order, (b) pseudo-second order and (c) Elovich kinetic plots for the adsorption of Pb (II) onto TSA@amine modified SiO₂.

(a) and (b) show nonlinear fit of pseudo-first and pseudo-second order models using the predicted q_t values, respectively. The values of pseudo first order rate constant (k_1) were found to be 0.046, 0.062, 0.107 and 0.201 min^{-1} at 300 , 305, 310 and 315 K, respectively which indicated that the uptake of Pb(II) increased with increasing temperature. On the other hand, the values of pseudo second order rate constant (k_2) varied over the range 0.002–0.006 g/mg/min as the temperature increased from 300 to 315 K.

It was observed that the values of R^2 were >0.990 for both pseudo-first order and pseudo second order kinetic models over the temperature range 300–315 K. The suitability of kinetic model cannot be decided on the basis of R^2values only. The capacities obtained from pseudo-first order model were 54.09, 56.94, 60.81 and 62.12 mg/g corresponding to 300, 305, 310 and 315 K, respectively and these values deviated from the experimentally determined adsorption capacities (49.01, 49.24, 49.51 and 49.73 mg/g corresponding to temperatures 300, 305, 310 and 315 K). On the other hand, the values of adsorption capacity computed from pseudo second order kinetic model were comparable at studied temperatures. Moreover, the values of error functions were very low for pseudo-second order model as compared to pseudo-first order model. Therefore, it is concluded that the uptake of Pb(II) on the heterogeneous surface of TSA@amine modified SiO₂ was accurately demonstrated by pseudo-second order model. Further, it is suggested that chemisorption is also involved in the uptake of Pb(II) ions.

To validate the uptake of Pb(II) onto heterogeneous surface of TSA@amine modified SiO₂ as a chemisorption process kinetic data were fitted to Elovich model (R^2 > 0.99). The nonlinear regression analysis of Elovich equation yielded the kinetic parameters and results are presented in Table 5. The nonlinear fitting of Elovich model is shown in Fig. 3c. Nonlinear regression of Elovich equation showed high values of $R^2$with low values of ARED, SSE, SAE and χ^2- over the temperature range 300–315 K which demonstrated the chemical nature of adsorption process.

3.5. Double-exponential model

Wilczak and Keinath (1993) have applied the double exponential model to explain the uptake of Cu(II) and Pb(II) onto activated carbon. This model suggested the involvement of two steps namely rapid and slow stages in the adsorption process. Rapid phase of the model is due to the external mass transfer of solute from bulk solution to the adsorbent surface where it interacts with the binding sites whereas slow stage is due to the intraparticle diffusion. Similarly, Rahman and Nasir (2020) have suggested that the uptake of acetaminophen by the adsorbent occurred in two stages which was validated by double exponential model. Double exponential model is expressed by Eq. (8):

$$q_t = q_e - \frac{D_1}{M} exp(-k_{D1}t) - \frac{D_2}{M} exp(-k_{D2}t) \tag{8}$$

where D_1 and K_{D1} are the rapidly adsorbed fraction of the solute (mg/L) and the rate constant of rapid step (min^{-1}), respectively. D_2 and K_{D2} are slowly adsorbed fraction of solute and rate constant of slow step of adsorption. M denotes the mass of adsorbent (g/L). The fraction of solute adsorbed in rapid and slow steps and their corresponding rate constants can be determined by the following assumption.

When $K_{D1} \gg K_{D2}$ then slow step contributes to overall kinetics and Eq. (8) is reduced to:

$$q_t = q_e - \frac{D_2}{M} exp(-k_{D2}t) \tag{9}$$

Eq. (9) can be linearized as:

$$ln(q_e - q_t) = ln\frac{D_2}{M} - k_{D2}t \tag{10}$$

The values of D_2 and KD_2 were computed from ln $(q_e - q_t)$ versus t plot. The values of D_1 and KD_1 can be calculated using Eq. (11):

$$ln\left(q_e - q_t - \frac{D_2}{M} exp^{-k_{D2}t}\right) = ln\frac{D_1}{M} - k_{D1}t \tag{11}$$

The values of KD_1 and KD_2 are not able to illustrate the exact quantification of the rapid and slow steps of the sorption. Therefore, the fraction of solute adsorbed in rapid (RF) and slow (SF) stages can be computed using Eqs. (12) and (13):

$$RF = \left(\frac{D_1}{D_1 + D_2}\right)100 \tag{12}$$

$$SF = \left(\frac{D_2}{D_1 + D_2}\right)100 \tag{13}$$

The kinetic parameters for both slow and rapid steps were determined from the plots of ln{q_e-q_t-(D_2/M)exp(-k_{D2} t)} vs t (Fig. 4) and presented in the Table 6. It was found that the D_1 increases whereas D_2 decreases with increasing temperature. The difference between the KD_2 (0.104–0.100) and KD_1 (0.110–0.121) is not high, indicating the importance of both slow and rapid steps at all temperatures. The values SF (37.120–30.432) and RF (62.026–69.568) confirmed that major fraction of Pb(II) was absorbed in the rapid step due to the interaction with the active sites available on the adsorbent surface. In the slow step, the intraparticle diffusion is involved in the adsorption process. From these observations, it was concluded that both chemical and physical interactions were responsible for adsorption of Pb(II) onto TSA@a-mine modified SiO_2. Similar results were reported for the adsorption of Th(IV) onto amino group functionalized titanosilicate (Milani and Karimi, 2017).

3.6. Thermodynamics of adsorption

Thermodynamic parameters for the uptake of Pb(II) onto TSA@amine modified SiO_2 were calculated using the values of thermodynamic equilibrium constant (k_c) at different temperatures. The values of $\Delta G°$, $\Delta H°$ and $\Delta S°$ were evaluated using Eqs. (14), (15) and (16) (Rahman and Varshney, 2020).

$$k_c = \frac{q_e}{C_e} \tag{14}$$

$$\Delta G^o = -RTlnk_c \tag{15}$$

$$lnk_C = \frac{\Delta S^0}{R} - \frac{\Delta H^0}{RT} \tag{16}$$

where R and T are the universal gas constant (8.314 J/mol/K) and temperature (Kelvin), respectively. The value of k_c can be calculated to become dimensionless by multiplying it by 1000 assuming the solution density $\approx$ 1 g/mL (Milonjic, 2007). The values of free energy change (ΔG^0) were found to vary from −9.388 to −13.089 kJ/mol over the temperature range 300–315 K. The values of $\Delta H°$ and $\Delta S°$ were computed from linear plot of lnk_C versus $\frac{1}{T}$ (Fig S2; Supplementary information). The positive values of enthalpy change ($\Delta H°$ = 65.381 kJ/mol) and entropy change ($\Delta S°$ = 0.249 k J/mol) indicated the endothermic nature of adsorption of Pb(II) onto TSA@amine modified SiO_2 and enhanced randomness at adsorbent/liquid interface.

4. Conclusions

The uptake of Pb(II) onto TSA@)amine modified SiO_2 was studied in batch mode and the value of q_e was 92.50 mg/g at 300 K. The equilibrium data fitted well to the Freundliuch isotherm model with $R^2 > 0.99$ and the value of q_e calculated from the model (92.45 mg/g) agrees well with the experimental value. Pseudo-second order model was found to be the best fit model which suggested the involvement of chemical reaction in adsorption process. Elovich model validated the chemisorption process because the kinetic data fitted well to Elovich model with $R^2 > 0.99$. Double exponential model indicated that the adsorption occurred in two stages; rapid stage involves the transport of solute from bulk solution to the surface of adsorbent to bind with the active sites and in the slow stage intraparticle diffusion takes place.
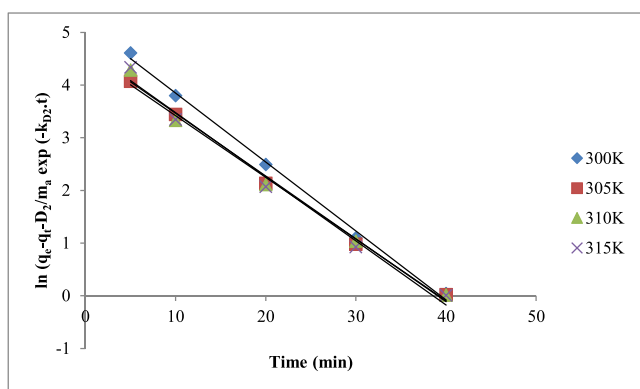

Fig. 4. Double exponential plots of ln{q_e-q_t-(D_2/M)exp(-k_{D2} t)} vs t.

Table 6
Parameters of double exponential modal for the adsorption of Pb (II) onto TSA@amine modified SiO_2.

Tmp. (K)	Parameters							
	Slow step				Rapid step			
	D_2 (mg/L)	KD_2 (min^{-1})	R^2	SF (%)	D_1 (mg/L)	KD_1 (min^{-1})	R^2	RF (%)
300	0.581	0.104	0.9980	37.120	0.949	0.110	0.9934	62.026
305	0.541	0.102	0.9950	35.780	0.971	0.116	0.9917	64.219
310	0.467	0.101	0.9920	32.207	0.983	0.117	0.9904	67.793
315	0.437	0.100	0.9921	30.432	0.999	0.121	0.9924	69.568

(C_0 = 50 mg/L; pH 6.0; adsorbent dose = 0.2 g; volume = 20 mL).

Declaration of Competing Interest

Acknowledgements

Appendix A. Supplementary data

Supplementary data to this article can be found online at https://doi.org/10.1016/j.jksus.2020.101232.

References

Almasian, A., Giahi, M., Fard, G.C., Dehdast, S.A., 2018. Removal of heavy metal ions by modified PAN/PANI-nylon core-shell nanofibers membrane: Filtration performance, antifouling and regeneration behavior. Chem. Eng. J. 351, 1166–1178. https://doi.org/10.1016/j.cej.2018.06.127.

Azmi, S.N.H., Al-Balushi, M., Al-Siyabi, F., Al-Hinai, N., Khurshid, S., 2020. Adsorptive removal of Pb(II) ions from groundwater samples in Oman using carbonized Phoenix dactylifera seed (Date stone).J. King Saud Univ. Sci. 32, 2931–2938. https://doi.org/10.1016/j.jksus.2020.07.015.

Badescu, I.S., Bulgariu, D., Ahmad, I., Bulgariu, L., 2018. Valorisation possibilities of exhausted biosorbents loaded with metal ions- a review. J. Environ. Manage. 224, 288–297.

Bulgariu, L., Bulgariu, D., 2018. Functionalized soy waste biomass – A novel environmental-friendly biosorbent for the removal of heavy metals from aqueous solution. J. Cleaner Prod. 197, 875–885.

Chen, H., Zhao, Y., Wang, A., 2007. Removal of Cu(II) from aqueous solution by adsorption onto acid-activated palygorskite. J. Hazard. Mater. 149, 346–356.

Chowdury, Z.Z., Hamid, S.B.A., Rahman, M.M., Rafique, R.F., 2016. Catalytic activation and application of micro-spherical carbon derived from hydrothermal carbonization of lignocellulosic biomass: statistical analysis using Box-Behnken design. RSC Adv. 6, 102680–102694.

Debnath, B., Singh, W.S., Manna, K., 2019. Sources and toxicological effects of lead on human health. Indian J. Med. Spec. 10, 66–71.

Fewtrell, L., Kaufmann, R., Pruss-Ustün, P., 2003. Lead: Assessing the environmental burden of disease at national and local levels, Geneva. World Health Organization (Environmental Burden of Disease Series No. 2, DOI.

Gupta, V.K., Singh, P., Rahman, N., 2004. Adsorption behavior of Hg (II), Pb (II) and Cd (II) on Duolite C-433: A synthetic resin. J. Colloid Interface Sci. 275, 398–402.

Ibrahim, T.N.B.T., Othman, F., Mahmood, N.Z., 2020. Baseline study of heavy metal pollution in a tropical river in a developing country. Sains Malaysiana 49, 729–742. https://doi.org/10.17576/jsm-2020-4904-02.

Joel, C., Bennie, R.B., Raj, A.N.P., David, S.T., Abraham, S.D., 2020. Removal of toxic metal ions by macroacyclic ligands via liquid-liquid extraction technique. Sep. Sci. Technol. https://doi.org/10.1080/01496395.2020.1774609.

Khammar, S., Bahramifar, N., Younesi, H., 2020. Optimization using the response surface methodology for adsorption of polychlorinated biphenyls (PCBs) from transformer oil bymagnetic CMCD-Fe3O4@SiO2 nanoparticles. Mater. Chem. Phys. 252,. https://doi.org/10.1016/j.matchemphys.2020.123195 123195.

Kumar, A., Kumar, A., Cabral-Ointo, M.M.S., et al., 2020. Lead toxicity: Health hazards, influence on food chain, and sustainable remediation approaches. Int. J. Environ. Res. Public Health 17, 2179. https://doi.org/10.3390/ijerph17072179.

Kumar, K.V., Sivanesan, S., 2006. Isotherm parameters for basic dyes onto activated carbon: comparison of linear and nonlinear method. J. Hazard. Mater. 129, 147–150.

Levin, R., Vieira, C.L.Z., Mordarski, D.C., et al., 2020. Lead seasonality in humans, animals, and the natural environment. Environ. Res. 180,. https://doi.org/10.1016/j.envres.2019.108797 108797.

Lutfullah, Rashid, M, Rahman, N, 2012a. Synthesis, characterization and sorption characteristics of a fibrous organic-inorganic composite material. Adv. Sci. Lett. 17, 136–142. https://doi.org/10.1166/asl.2012.3691.

Lutfullah, Rashid, M, Rahman, N, 2012b. Zirconium(IV) phosphosulphosalicylate as an important lead(II) selective ion-exchange material: Synthesis, characterization and adsorption study. Adv. Sci. Lett. 17, 184–190.

Milani, S.A., Karimi, M., 2017. Isotherm, kinetic and thermodynamic studies for Th (IV) sorption by amino group-functyionalizedtitanosilicate from aqueous solutions, Korean. J. Chem. Eng. 34, 1159–1169.

Milonjic, S.K., 2007. A concidration of the correct calculation of thermodynamic parameters of adsorption. J. Serb. Chem. Soc. 72, 1363–1367.

Qin, H., Hu, T., Zhai, Y., et al., 2020. The improved methods of heavy metals removal by biosorbents: A review. Environ. Pollut. 258,. https://doi.org/10.1016/j.envpol.2019.113777 113777.

Rahman, N., Haseen, U., 2014. Equilibrium modeling, kinetic and thermodynamic studies on adsorption of Pb (II) by a hybrid inorganic-organic material: Polyacrylamide zirconium (IV) iodate. Ind. Eng. Chem. Res. 53, 8198–8207.

Rahman, N., Haseen, U., 2015. Development of polyacrylamide chromium oxide as a new sorbent for solid phase extraction of As (III) from food and environmental water samples. RSC Adv. 5, 7311–7323.

Rahman, N., Haseen, U., Khan, M.F., 2015. Cyclic tetra [(indolyl)-tetramethyl]-diethane-1,2-diamine (CTet) impregnated hydrous zirconium oxide as a novel hybrid material for enhanced removal of fluoride from water samples. RSC Adv. 5, 39062–39074.

Rahman, N., Khan, M.F., 2015. Development of poly-o-toluidine zirconium (IV) ethylenediamine as a new adsorbent for nitrate: Equilibrium modeling and thermodynamic studies. J. Ind. Eng. Chem. 25, 272–279.

Rahman, N., Khan, M.F., 2016. Nitrate removal using poly-o-toluidine zirconium (IV) ethylenediamine as adsorbent: Batch and fixed-bed column adsorption modeling. J. Water Process Eng. 9, 254–266.

Rahman, N., Haseen, U., Rashid, M., 2017. Synthesis and characterization of polyacrylamide zirconium(IV) iodate ion- exchanger: Its application for selective removal of lead(II) from wastewater, Arabian. J. Chem. 10, S1765–S1773.

Rahman, N., Nasir, M., 2017. Development of Zr(IV) – doped polypyrrole/zirconium (IV) iodate composite for efficient removal of fluoride from water environment. J. Water Process Eng. 19, 172–184.

Rahman, N., Nasir, M., 2018. Application of Box-Behnken design and desirability function in the optimization of Cd (II) removal from aqueous solution using poly (o-phenylenediamine)/hydrous zirconium oxide composite: equilibrium modeling, kinetic and thermodynamic studies. Environ. Sci. Pollute. Res. 25, 26114–26134.

Rahman, N., Nasir, M., 2019.N-(((2-((2-aminoethyl)amino)ethyl)amino)methyl)-4-sulfamoylbenzamide impregnated hydrous zirconium oxide as a novel adsorbent for removal of Ni(II) from aqueous solutions: Optimization of variables using central composite design. ACS Omega, 4, 2823-2832.

Rahman, N., Khan, M.F., Nasir, M., 2020. Experimental design approach for optimization of Pb(II) removal from aqueous solution using poly-o toluidine/ stannic(IV) triethanolamine as adsorbent. Environ. Technol. Innovat. 17, 100634.

Rahman, N., Nasir, M., 2020. Facile Synthesis of thiosalicylic acid functionalized silica gel for effective removal of Cr (III): Equilibrium modeling, kinetic and thermodynamic studies. Environ. Nanotechnol. Monit. Manag. 14, https://doi.org/10.1016/j.enmm.2020.100353 100353.

Rahman, N., Nasir, M., 2020. Effective removal of acetaminophen from aqueous solution using Ca (II)-doped chitosan/β-cyclodextrincomposite. J. Mol. Liq. 301, 112454.

Rahman, N., Varshney, P., 2020. Assessment of ampicillin removal efficiency from aqueous solution by polydopamine/zirconium (IV) iodate: Optimization by response surface methodology. RSC Adv. 10, 20322–20337.

Rao, J.V., Vengamma, B., Naveen, T., Naveen, V., 2014. Lead encephalopathy in adults. J. Neurosci. Rural Pract. 5, 161–163.

Sujatha, S., Venkatesan, G., Sivarethinamohan, R., 2020. Optimization of lead removal in exhausting *Manilkarazapota* based activated carbon: Application of response surface methodology. Environ. Technol. 41, 2478–2493. https://doi.org/10.1080/09593330.2019.1570347.

Tang, X., Zheng, H., Teng, H., Sun, Y., Guo, J., Xie, W., Yang, Q., Chen, W., 2016. Chemical coagulation process for the removal of heavy metals from water: A review. Desalination Water Treat. 57, 1733–1748. https://doi.org/10.1080/19443994.2014.977959.

Thaci, B.S., Gashi, S.T., 2019. Reverse osmosis removal of heavy metals from wastewater effluents using biowaste materials pretreatment. Pol. J. Environ. Stud 28, 337–341. https://doi.org/10.15244/pjoes/81268.

Wilczak, A., Keinath, T.M., 1993. Kinetics of sorption and desorption of copper (II) and lead (II) on activated carbon. Water Environ. Res. 65, 238–244.

Zhou, Q., Yang, N., Li, Y., et al., 2020. Total concentrations and sources of heavy metal pollution in global river and lake water bodies from 1972 to 2017. Glob. Ecol. Conser. 22, 00925. https://doi.org/10.1016/j.gecco.2020.e00925.